https://doi.org/10.5194/egusphere-2025-6112
Preprint. Discussion started: 30 March 2026

Short communication: Crystalline features of fission tracks in monazite: Evidence from swift heavy ion irradiation and transmission electron microscopy

Shoma Fukuda[1], Norito Ishikawa[2], Toru Nakajima,[3] Hiroaki Ogawa[2], Tomitsugu Taguchi[4]
[1] Tono Geoscience Center, Japan Atomic Energy Agency (JAEA), Toki, Gifu 509-5102, Japan
[2] Nuclear Science and Engineering Center, Japan Atomic Energy Agency (JAEA), Tokai, Ibaraki 319-1195, Japan
[3] School of Sustainable Design, University of Toyama, Gofuku, Toyama 930-8555, Japan,
[4] Foundational Quantum Technology Research Directorate, National Institutes for Quantum Science and Technology (QST), Takasaki, Gunma 370-1292 Japan

Correspondence to: Fukuda Shoma (fukuda.shoma@jaea.go.jp)

Abstract. To further understand monazite fission-track thermochronometry, three experiments were conducted. 1) Cretaceous monazite-(Ce) was irradiated with 80 and 200 MeV Xe ions using a tandem accelerator. Transmission electron microscopy (TEM) was then used to define crystalline structures of spontaneous fission tracks in monazite. 2) Zircon powder was irradiated with 80 MeV Xe ions. TEM was subsequently used and the results were compared with those obtained from monazite. 3) Quaternary monazite-(Ce) in a resin mount was irradiated with 80 MeV Xe ions. Next, chemical treatment (etching) was performed to ascertain etchability of the ion tracks in monazite. These irradiation conditions correspond to the energies of heavily charged particles of spontaneous fission and the entire spontaneous fission event. This experiment simulated the damage process associated with spontaneous fission. First, from the TEM images of ion-irradiated Cretaceous monazite, ion track damage could be visualized as a low-density columnar region where the crystal lattice was maintained, and no sign of amorphization for both energies was observed. These results suggest that point defects accumulate around the ion path in monazite, in contrast to the amorphous features in zircon under the same irradiation conditions. Secondly, these etching experiments on ion-irradiated Quaternary monazite indicate that even non-amorphous domains can be selectively etched, which is consistent with previous studies on etching ion tracks in non-amorphous materials, as well as natural fission tracks and alternative ion tracks on monazite. These observations suggest that etchability of fission tracks in monazite is likely attributable to accumulated point defects rather than to amorphous regions. Hence, estimation of ultra-low closure temperature in the monazite fission track system should be derived from the formation of point defects rather than from amorphous regions, since the former can be easily annealed compared to the latter.

https://doi.org/10.5194/egusphere-2025-6112
Preprint. Discussion started: 30 March 2026

1 Introduction

Monazite (LREE(PO_4)) is a phosphate mineral composed mainly of light rare earth elements and is found in igneous, metamorphic, and sedimentary rocks. Monazite is useful for geochronologic investigations due to the presence of relatively high U and Th contents. The monazite fission-track (MFT) method has emerged as a promising new thermochronometer in the ultra-low temperature range (e.g., Gleadow et al., 2002). The estimated closure temperature is less than 50°C, according to results from short-term annealing experiments of Kr ion tracks (Weise et al., 2009) and Cf fission fragment tracks (Jones et al., 2021). The MFT method has the potential to facilitate a more comprehensive understanding of the thermal history of the earth's crust, particularly in shallower depths of 1 km or less.

MFT dating is an evolving method, requiring fundamental research over the past two decades. Weise et al. (2009) initially verified the closure temperature of the MFT system based on Kr ion irradiation and short-term annealing and etching experiments. Jones et al. (2021) conducted ion-track annealing experiments using Cf fragments at various heating temperatures between 30 and 400°C and durations (1−1000 hours) to estimate the thermal annealing process. Based on these studies, the potential of MFT as an ultra-low thermochronometer at 25−50°C was identified. Jones et al. (2019) proposed ideal etching conditions of 6M HCl at 90°C for 60−90 min as the basis for MFT dating. This etching recipe enables the enlargement of fission tracks and observation with an optical microscope. Based on Raman spectroscopic analysis and stepwise etching experiments using monazite from Japanese rock samples of various ages, Nakajima et al. (2024) demonstrated that etching durations vary from 90 to 1200 min due to the degree of radiation damage. This study also contributed to determining that longer etching durations are necessary for monazite with little radiation damage (i.e., samples with young formation age or low U-Th concentrations), and step-etching is useful for such samples. Initially, MFT dating accompanied with length distributions was applied to geological samples by combining apatite FT ages and apatite and zircon (U-Th)/He ages (Jones et al., 2023; Jepson et al., 2025). However, for practical implementation of the MFT method in geologic studies, challenges still remain, primarily due to the limited understanding of certain constants in the age equation (e.g., initial length of spontaneous MFT) and long-term annealing behavior. To further understand the fundamental parameters and annealing kinetics of MFT systems, investigation of the mechanism of fission track formation and the annealing processes is needed.

As previously mentioned, short-term annealing experiments using ion tracks have been previously conducted, but conventional studies involving short-term annealing experiments using induced ^{235}U tracks have not been carried out. Although induced fission of ^{235}U typically forms induced tracks through thermal neutron irradiation, the light

https://doi.org/10.5194/egusphere-2025-6112
Preprint. Discussion started: 30 March 2026

REE-rich nature of monazite has been reported to cause Gd to shield thermal neutrons, and as a result, generating heat and creating induced tracks, as well as microscopy, are difficult (Gleadow et al., 2002). Although the preceding study considered short heating experiments using ion tracks, it should be noted that the behaviors exhibited by ^{235}U induced tracks and ion tracks may not be directly analogous, making comparison of the results difficult. Notably, the experiment conducted by Weise et al. (2009) investigated the annealing process using Kr ion tracks at 300 MeV, which is significantly higher in energy compared to spontaneous fission. Seydoux-Guillaume et al. (2004) demonstrated that monazite from all four samples of various ages ranging from 24 to 1900 Ma displayed lattice distortions (lattice defects) that accumulated with age, but also lacked amorphous areas. This observation could be explained by radiation damage recovery by self-irradiation (Nasdala et al., 2020) as well as thermal annealing over the geologic timescale. In another research, 14 MeV Au ion irradiation was adopted for Eu-doped monazite-(La), which implied the tendency that monazite would recrystallize (Gilson et al., 2024). Up to now, formation of fission tracks in monazite through spontaneous fission has remained a subject of limited understanding, primarily due to the paucity of investigations conducted on the characteristics of latent tracks in monazite. Furthermore, the processes of radiation damage recovery and the annealing of FTs in monazite are not yet fully understood. In the case of other accessory minerals of fission-track thermochronometers, such as apatite or zircon, TEM observations to examine the annealing behaviors have been carried out (e.g., Yada et al., 1987; Li et al., 2011). However, research on the formation or annealing behavior of MFTs using TEM observation could not be found,.

This study aims to deepen understanding of the formation and annealing processes in the MFT system. In order to further investigate those elementary processes related to MFT formation/annealing, natural monazite-(Ce) was irradiated with Xe ions at energies simulating spontaneous fission. Transmission electron microscopic (TEM) observations were carried out to ascertain potential formation of amorphous areas, based on the prevailing consensus that fission tracks in minerals are amorphous (see also the review by Tagami and O'Sullivan, 2005). To compare the results with those obtained for monazite, zircon, which is a well-known target mineral for fission track dating, was also exposed to Xe ion irradiation and then subjected to TEM observation under the same conditions. Observation of the crystal structure of ion tracks in monazite can provide crucial fundamental information in the understanding of elementary processes. Greater comprehension of properties inherent to MFTs is expected to lead to significant advancements in fundamental research, leading to the establishment of annealing kinetics.

https://doi.org/10.5194/egusphere-2025-6112
Preprint. Discussion started: 30 March 2026

2 Materials and methods：Xe irradiation and TEM observations

The following three types of samples were used in this study: Cretaceous monazite-(Ce) separated from a rock specimen EY137-21, Quaternary monazite-(Ce) from Toya-6b tephra, and zircon powder. EY137-21 was obtained from Kibe granite, Cretaceous granite of the Ryoke Belt in the Southwest Japan Arc. This particular sample was used by Nakajima et al. (2024), collected from a riverbed approximately 100 meters east of EY137A, which was previously sampled by Skrzypek et al. (2016) and Jones et al. (2023). Toya-6b was obtained from the Quaternary Toya ignimbrite, a siliciclastic eruptive deposit comprised of pumiceous beds and lag deposits from the Toya caldera at approx. 0.1 Ma (Tomiya and Miyagi, 2020). This deposit is the uppermost layer in the six subdivided flow units described by Goto et al. (2018). It should be noted that Nakajima et al. (2024) reported that monazite from the fifth layer showed little radiation damage based on Raman spectrometry. Monazite crystals of Toya-6b were obtained by separating them from the pumice. In this study, commercial zircon powder ($ZrSiO_4$, 98%) was used, purchased from Kojundo Chemical Laboratory Co., Ltd., Saitama, Japan.

Monazite grains were extracted from rock samples using conventional heavy-liquid and magnetic separation techniques. The rock samples were first crushed and then sieved through a 60-mesh sieve to collect the remaining particles. Heavy mineral fraction was extracted using the general heavy-liquid separation method with a sodium polytungstate (SPT) solution (specific gravity 3.06 g/cm³). The fraction then subjected to magnetic separation using a neodymium magnet. A ferrite magnet was also used to remove ferromagnetic minerals from the magnetic fraction, and monazite crystals were hand-picked and separated. Crystal selection was based on the following criteria: (1) semi-authigenic to authigenic shapes (i.e., monoclinic system), (2) opaque lemon yellow color or colorless, and (3) widths ranging from >50 to 100 microns.

For ion-irradiation experiments, EY137-21 monazite and zircon powder were finely ground using an agate pestle and mortar to prepare thin samples suitable for TEM observation. The ground samples were dispersed in ethanol by an ultrasonic bath for several minutes. Thereafter, the ethanol was dripped onto 3 mm diameter 200 mesh copper grids covered with porous carbon films. Subsequently, the grids were air-dried at room temperature. For the etching experiment following ion irradiation, Toya-6b monazite was mounted in epoxy resin, and then ground and polished using standard procedures to ensure a flat surface for irradiation and microscopy. EY137-21 monazite was irradiated with 80 MeV and 200 MeV Xe at room temperature using a tandem accelerator at JAEA-Tokai, while the zircon powder and the Toya-6b monazite mount were irradiated with 80 MeV Xe ions. All irradiations were performed perpendicular to the grid surface. The ion energies used in this study (80 MeV and 200 MeV) are commensurate with the initial energy of fission fragments from spontaneous fission (~70 MeV) and the total energy

https://doi.org/10.5194/egusphere-2025-6112
Preprint. Discussion started: 30 March 2026

of the spontaneous fission event (~170 MeV), as previously described by Weise et al. (2009). The ion fluences were in the range from 1 to 3 × 10^{11} ions/cm^2, which is sufficient to allow observation of individual tracks. The ion-irradiated domains were examined using a TEM (JEOL Ltd., 2100F, Japan) operated at 200 kV, excluding the Toya-6b monazite. Instead of TEM observation, Toya-6b monazite was subjected to step-etching and then microscopy to verify etchability of ion tracks after Xe ion irradiation. Step-etching was carried out following the procedures described by Nakajima et al. (2024), based on Jones et al. (2019). The original etching time reported in Jones et al. (2019) was 60–90 min, as required to visualize the tracks. However, Nakajima et al. (2024) also suggested that etching time varied depending on the level of radiation damage in the crystal grain. In this study, etching duration for Toya-6b monazite was set at 90 and 450 min to verify the step-etching process after ion irradiation.

3 Results and interpretations

3.1 TEM observations of the Cretaceous monazite and zircon

As illustrated in Figs. 1–3, the examination results of regions exposed to 80 MeV and 200 MeV Xe ions on natural monazite-(Ce) are presented. Cross-sections of Xe ion tracks in EY137-21 monazite exhibit rectangular shapes with approximate lengths of 5 and 3 nm. Furthermore, color tone of the irradiated domain in Figs. 1 and 2 changes from bright to dark contrasts when shifted from underfocus to infocus and overfocus, indicating a low-density structure that can be visualized as Fresnel contrast. The irradiated domains for both energy levels (80 and 200 MeV) showed decreased density. In the magnified image of the irradiated domains, the crystalline lattices were preserved at both energies, and discernible amorphous areas were absent. The formation of low-density domains implies the formation of atomic vacancies, e.g., point defects, within the crystal lattice. In the TEM images of Xe ion irradiation with a 45-degree angle to the surface (Fig. 3), ion tracks exhibited linear patterns along the ion paths, as well as Fresnel contrast characterized by flickering contrasts in black and white, depending on the focus condition. This observation demonstrates that structural disorders are retained along the ion tracks. Notably, the ion tracks appear as intermittent lines with sufficient length, similar to the annealed tracks affected by the track segmentation process (e.g., Yamada et al., 1995; Li et al., 2011). This observation suggests that the recovery of ion tracks may occur in an erratic manner.

In contrast to the results observed in monazite, amorphous domains were observed in zircon irradiated with 80 MeV Xe ions (Fig. 4). As illustrated in Figs. 4(a) and 4(b), the ion tracks in zircon exhibited circular cross-sections with a diameter of approx. 5 nm. The damaged domains manifest an amorphous phase. As illustrated in Fig. 4(c),

https://doi.org/10.5194/egusphere-2025-6112
Preprint. Discussion started: 30 March 2026

linear structures are discernible in the TEM images in a slanted direction, indicating that amorphous regions are formed along the ion paths. Previous studies using ion irradiation and subsequent TEM observations have reported amorphous regions in zircon (e.g., Li et al., 2011), which is consistent with the results of this study. This incongruency in observation of ion track features between monazite and zircon is attributable to the difference in amorphizability of these minerals.

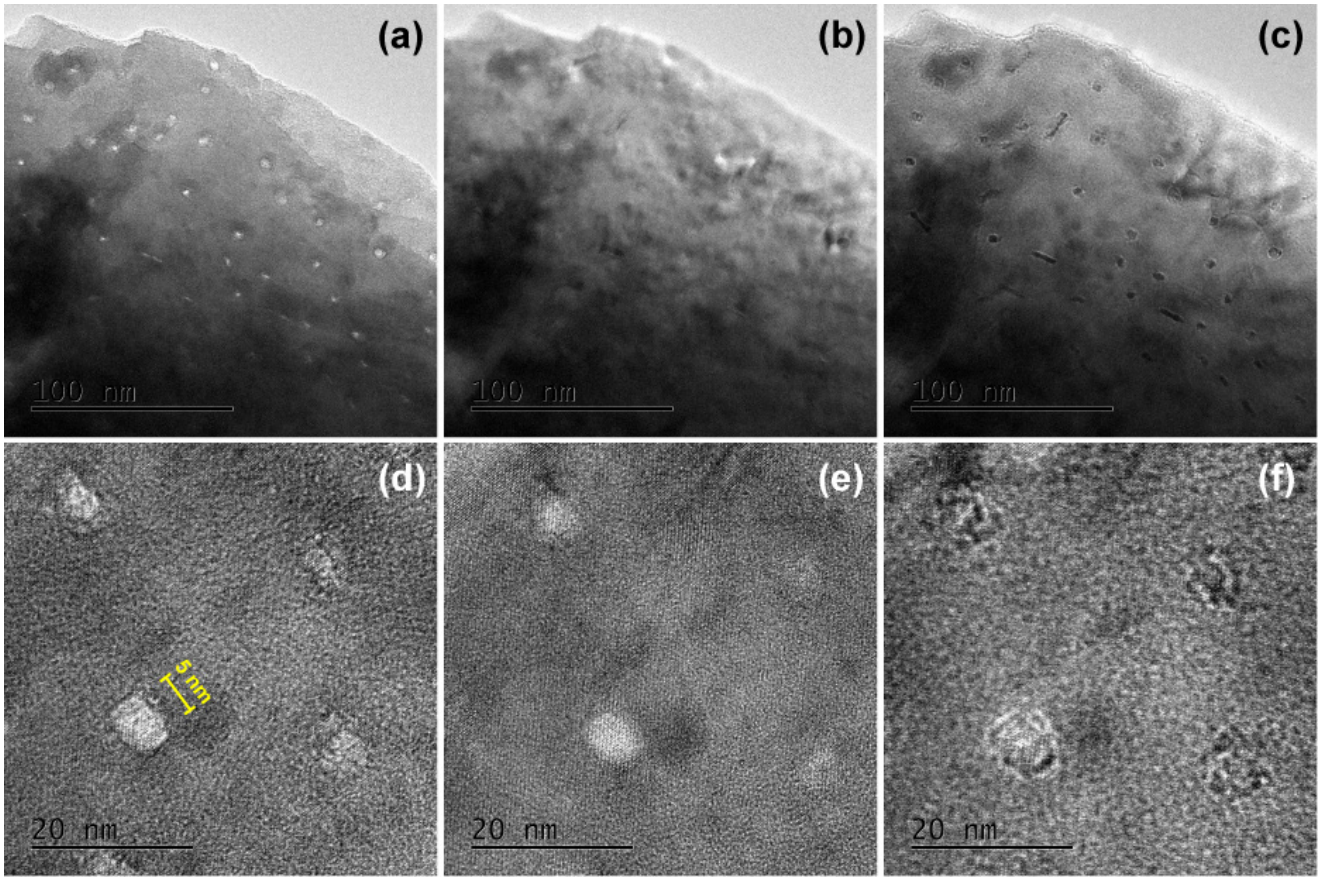

Fig. 1: Bright-field TEM images of EY137-21 monazite-(Ce) sample irradiated with 80 MeV Xe at 3×10^{11} ions/cm^2. (a)–(c) and (d)–(f) are in the same observation area. These photos are exhibited in (a, d) underfocus, (b, e) just infocus, and (c, f) overfocus conditions. Rectangle areas show where Xe ions were irradiated, and these structures are approximately 5 × 3 nm .

https://doi.org/10.5194/egusphere-2025-6112
Preprint. Discussion started: 30 March 2026

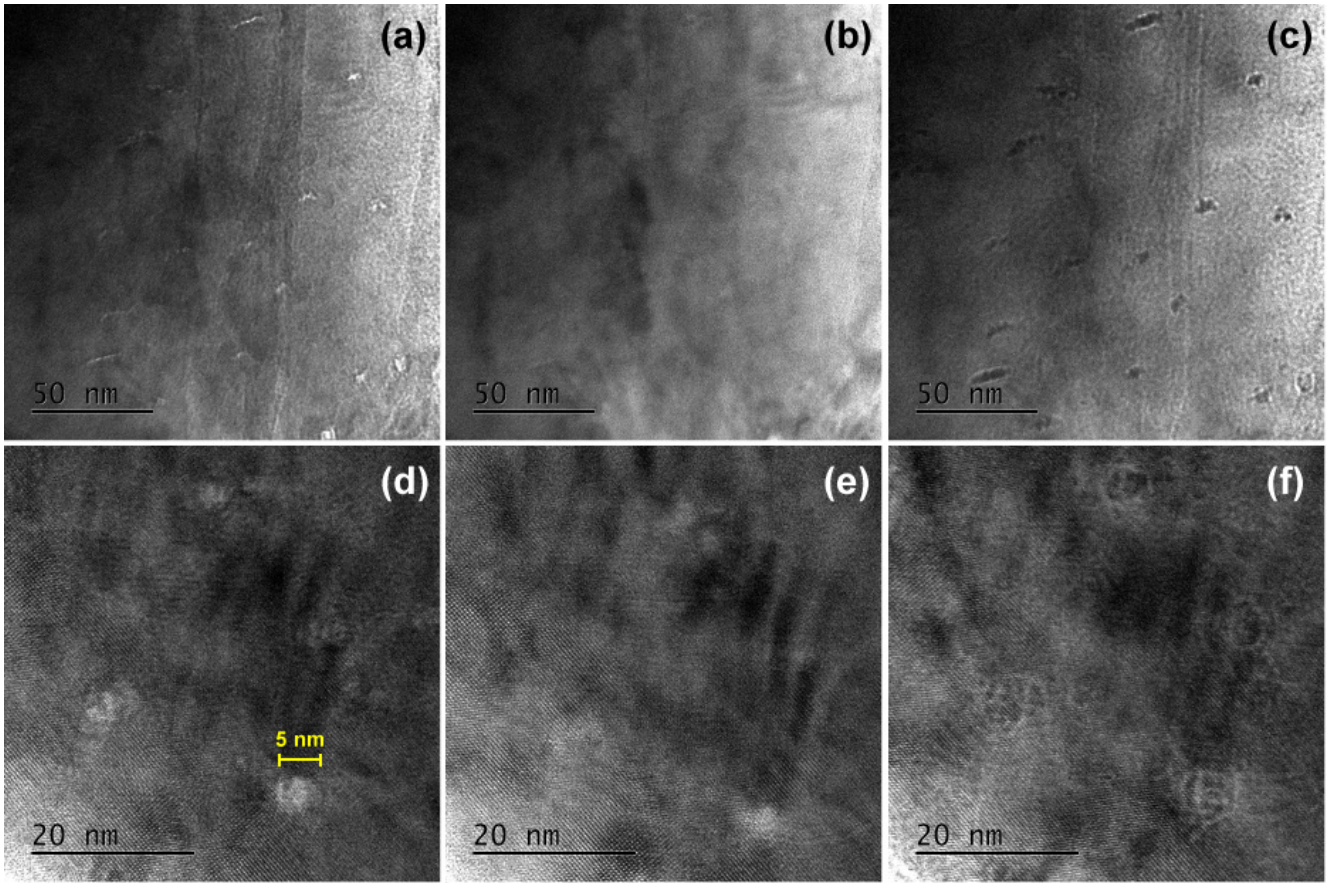

Fig. 2: Bright-field TEM images of EY137-21 monazite-(Ce) sample irradiated with 200 MeV Xe at 1×10^{11} ions/cm^2. (a)–(c) and (d)–(f) are in the same observation area. These photos are exhibited in (a, d) underfocus, (b, e) just or nearly infocus, and (c, f) overfocus conditions. Rectangle areas show where Xe ions were irradiated, and these structures are approximately 5×3 nm .

https://doi.org/10.5194/egusphere-2025-6112
Preprint. Discussion started: 30 March 2026

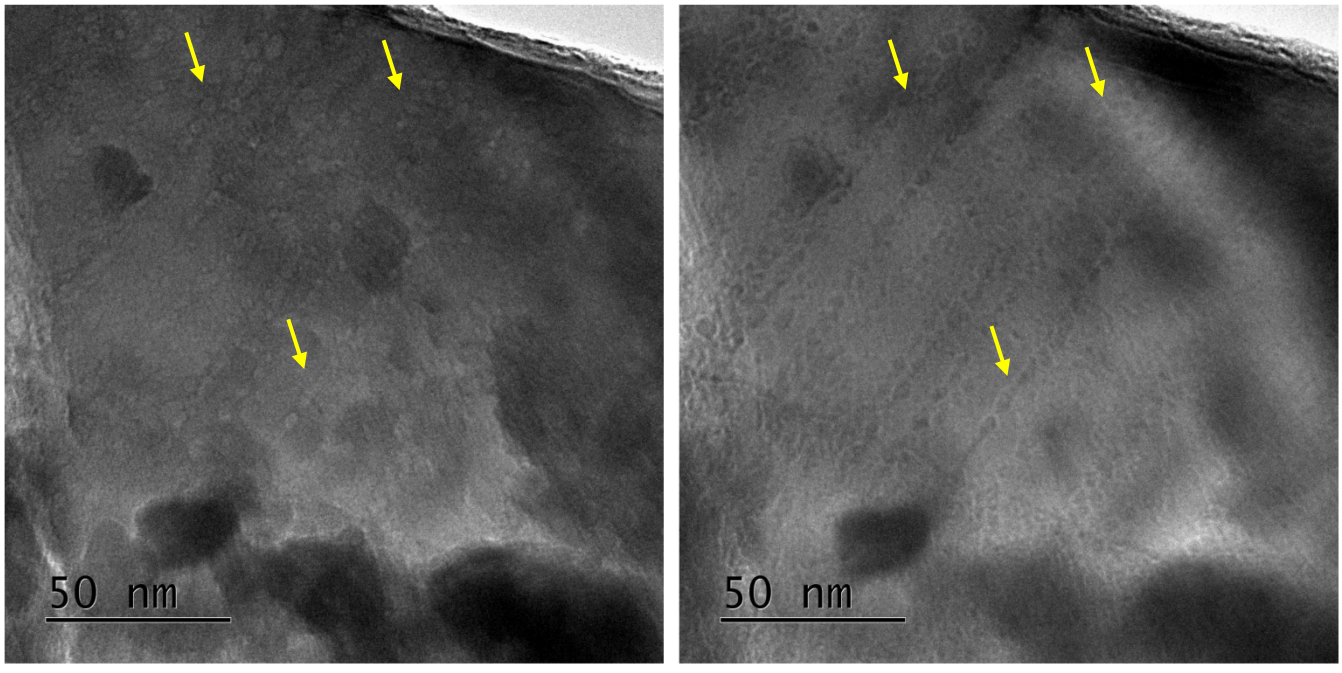

Fig. 3: Bright-field TEM images of EY137-21 monazite-(Ce) with the tilted irradiation of 80 MeV Xe at 3×10^{11} ions/cm^2 with 45-degree angle to the surface. The left image is captured in under-focus, while the right image is in over-focus. Linear structures with intermittent contrasts in light and dark colors in each focus condition indicate structural disorders resulting from ion irradiation. These yellow arrows in grains illustrate several examples of linear structures, which appear to be affected by track segmentation (e.g., Yamada et al., 1995; Li et al., 2011).

https://doi.org/10.5194/egusphere-2025-6112
Preprint. Discussion started: 30 March 2026

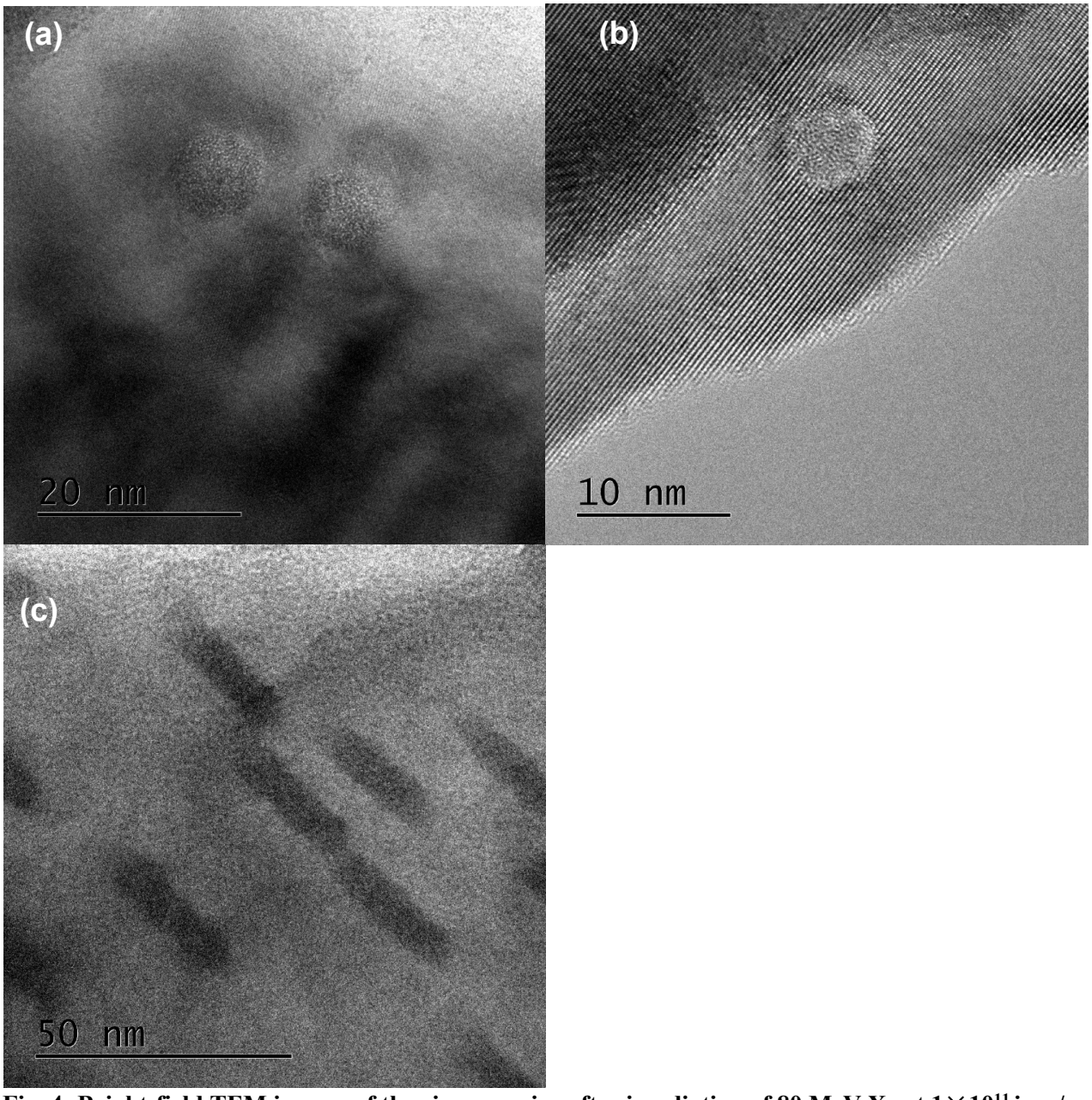

Fig. 4: Bright-field TEM images of the zircon grains after irradiation of 80 MeV Xe at 1×10^{11} ions/cm^2. (a) and (b) were captured in the normal (vertical) TEM observation, showing that the irradiated domains indicate circular shapes, and those inside are amorphous structures in both images. (c) was captured with a tilted observation from the grain surface. The irradiated domains show linear structures with elliptical shapes.

https://doi.org/10.5194/egusphere-2025-6112
Preprint. Discussion started: 30 March 2026

3.2 Etching experiments on ion tracks on the Quaternary monazite

In order to verify the etchability of ion tracks, a chemical etching procedure was performed on the irradiated Toya-6b monazite using 80 MeV Xe ions. Photomicrographs of etching at 90 min and 450 min after Xe ion irradiation procedure are shown in Fig. 5. With regard to the etching results for 90 min, no ion tracks were detected, while a substantial number of tracks were successfully etched after 450 min. The results of this study indicated that the Toya-6b monazite should exhibit minimal radiation damage, resulting in enhanced etching resistance. Nakajima et al. (2024) also reported results of etching spontaneous fission tracks in Toya-5b, the lower unit of Toya-6b. Toya-5b monazite could be successfully etched for a duration ranging from 500 to 1200 min, with significant variations observed among the grains. This outcome is similar to the etching of ion tracks in Toya-6b monazite, suggesting a comparable etching behavior in both specimens. Consequently, ion tracks can be etched selectively, despite their non-amorphous nature.

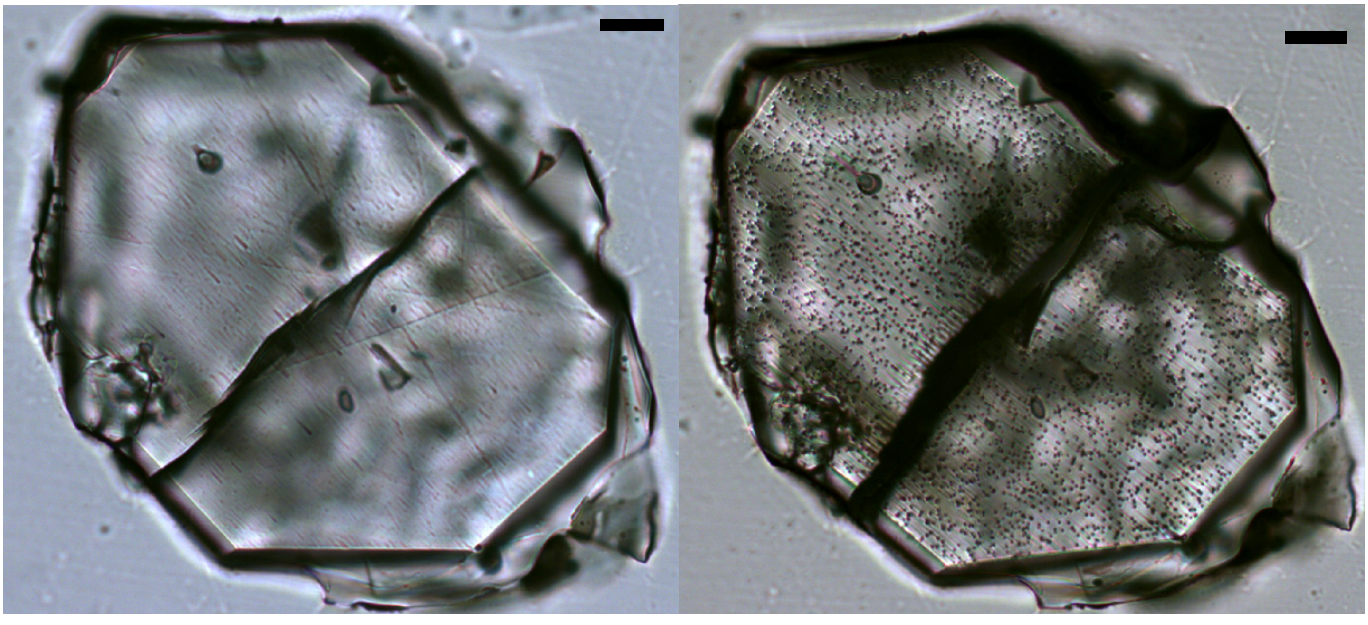

Fig. 5: Microscope images of the etched Quaternary monazite grain of Toya-6b, irradiated with 80 MeV Xe ions. All scale bars denote 10 µm. These images show the identical grain of Toya-6b after 90 min of etching (left) and after 450 min of etching (right). No etched ion tracks are observed in the left image, while numerous etched ion tracks are observed in the right one.

https://doi.org/10.5194/egusphere-2025-6112
Preprint. Discussion started: 30 March 2026

4 Discussion

4.1 Non-amorphizable nature of ion-irradiated monazite-(Ce)

Whether ion tracks in monazite-(Ce) subjected to fission fragments amorphize must be considered when formulating arguments regarding track formation and annealing processes. From the TEM observations, crystalline lattices in monazite-(Ce) are found to remain even after the Xe ion irradiation. The presence of lattice structures inside the ion tracks indicates a non-amorphizable nature of the ion tracks in monazite-(Ce). Similarly, the presence of such lattice structures inside ion tracks has been reported in ion tracks in synthetic monazite-(Sm) irradiated with 1.1 GeV Au ions (Overstreet et al., 2022). Since the regions penetrated by ion tracks are considered to have been amorphized, such discrepancy must be reconciled. The authors concluded that the TEM images, decrease in XRD peaks, and decrease in Raman peaks revealed the amorphization of the ion tracks. However, the presence of lattice structures inside the ion tracks in synthetic monazite-(Sm) has been observed. A decrease in XRD peak intensity and broadening can also occur due to disorder introduced within the crystal lattice in typical non-amorphizable CeO_2 (Ishikawa et al., 2008). Although the decrease in XRD and Raman peak intensity may serve as indirect evidence of amorphization, this is not a sufficient condition to prove amorphization. The experimental conditions previously outlined in the analogue of spontaneous fission are reiterated here. It is already known that species and energy of ion beams are controlling factors in the formation of ion tracks. In this regard, the electronic stopping power of Au ion irradiation is much higher than that of Xe ion. Furthermore, the kinetic energy of fission fragments is in the order of 70–100 MeV, which is much lower than 1.1 GeV. For all these reasons, the present experimental conditions (i.e., 80 MeV Xe ion irradiation) are considered appropriate in simulating the radiation damage of fission fragments. The TEM results of this study clearly indicate the non-amorphizable nature (rather than amorphizable nature) of the ion tracks in monazite-(Ce) subjected to fission fragments. Therefore, crystalline structures in monazite-(Ce) are retained in areas where spontaneous fission has occurred. Consequently, monazite-(Ce) can be considered a non-amorphizable material since it does not exhibit the characteristics of amorphous materials when exposed to fission fragment radiation. It should be noted that if monazite-(Sm) were an amorphizable material in these conditions, the possible effects of variation in chemical compositions between monazite-(Ce) and monazite-(Sm) should be examined, even though both are classified within the monazite group.

Monazite-(Ce) has been classified as a non-metamict crystal, as no amorphization is detected in natural samples. This phenomenon can be partially attributed to the process of damage recovery resulting from self-irradiation

https://doi.org/10.5194/egusphere-2025-6112
Preprint. Discussion started: 30 March 2026

caused by α-decay of U and Th contents abundant in monazite (e.g., Nasdala et al., 2020). Nasdala et al. (2020) examined three types of monazite-(Ce) (synthetic monazite, unheated, and annealed natural monazites) and subjected them to He ions at 7.7 MeV, followed by analysis using Raman and infrared spectroscopy. According to the results, unheated natural monazites exhibited alpha-particle-induced annealing of radiation damage in the high-damage-accumulation regime. This finding implies alpha-assisted crystallization, a process in which accumulated damage is partially annealed by alpha-particle irradiation. Conversely, Nasdala et al. (2020) proposed that additional damage accumulates due to He irradiation in synthetic and annealed monazites within the low-damage accumulation regime. This suggests that alpha-particle irradiation can induce radiation damage when the level of damage accumulation is low. In response to the proposed mechanism regarding the absence of metamict monazite, this study suggests that monazite is originally a non-amorphizable material. Specifically, monazite crystals can immediately recrystallize after spontaneous fission (see Sect. 4.2 for details). This implies that crystalline lattices are maintained throughout fission events even in the absence of self-irradiation (alpha-particle irradiation).

4.2 Formation mechanism and etchability of ion tracks in non-amorphizable materials

The principle mechanism of ion track formation is the thermal spike model, as proposed by Szenes (2011) and Toulemonde et al. (2012). According to the model, a rise in transient temperature near the ion path causes local melting along the path. In amorphizable materials, quenching the molten zone results in amorphization during rapid cooling. In non-amorphizable materials, however, although similar local melting occurs, the molten zone recrystallizes during rapid cooling. Recrystallization is described as the process by which atoms from the molten region move to their equilibrium positions at the interface with the crystalline structure (Ishikawa et al., 2017; Rymzhanov et al., 2019). The following discussion examines the formation process of ion tracks in monazite, incorporating previous investigations on non-amorphous materials.

In experiments using LiF crystals, exposure to high-energy Xe, Pb, Kr, and other ions was conducted, but amorphous areas were not detected (Trautmann et al., 1998). In an experiment using CeO_2 crystals, which are non-amorphized material, were irradiated with a 200 MeV Xe beam. Subsequent TEM observations confirmed that amorphization did not occur in the irradiated areas, and point defects arranged linearly along the ion trajectory (Takaki et al., 2016). These observations suggested that ion tracks are not amorphous and that the crystalline structure is predominantly maintained while crystalline strain accumulates near the ion path. Similarly, amorphous regions were not observed by TEM microscopy for monazite. After ionized fission fragments pass through monazite, the damaged areas may undergo repair during quenching or subsequent self-irradiation, as has been observed in non-amorphizable materials. Following the passage of charged fission fragments, a rapid increase in

https://doi.org/10.5194/egusphere-2025-6112
Preprint. Discussion started: 30 March 2026

temperature due to atomic interactions causes the linear ion tracks to melt. Because non-amorphizable materials have a high recrystallization capability, rapid recrystallization may occur in monazite during the rapid cooling of the melt.

Regarding etchability in non-amorphizable materials, chemical etching of ion tracks is known to show the line structure in LiF crystals (Trautmann et al., 1998). Irradiated domains in LiF are selectively etched along linear point defects formed by ion penetrations, a consequence of imperfect recrystallization of the melt. The presence of residual damage near the ion path can enhance the etching rate relative to that of the bulk material. Thus, remaining radiation damage (e.g., point defects formed in the lattice) can be selectively etched in non-amorphizable materials, even if the damaged region does not become amorphous. This study found no evidence of amorphous areas in monazite by TEM observation. However, the presence of linear damage areas could be confirmed through etching of monazite-(Ce) (Fig. 5; Weise et al., 2009; Jones et al., 2019, 2021, 2023; Nakajima et al., 2024). This study suggests that low-density regions may indicate the formation of point defects (e.g., atomic vacancies) within the crystal lattice. Consequently, according to TEM observation of the modified crystal structure of monazite-(Ce), linear point defects are suggested to be present near the ion paths. Furthermore, experimental findings derived from etching investigations subsequent to ion irradiation have also demonstrated that point defects can be selectively etched through the implementation of chemical treatments.

4.3 Why the monazite fission track system has an ultra-low closure temperature

Closure temperature of the zircon FT (ZFT) system on geologic timescales (1–10 Myr) is significantly higher (250–350°C; reviewed in Ketcham, 2019) than that of the MFT system. This disparity in closure temperature can be attributed to the difference in activation energy for annealing amorphous and non-amorphous tracks. The different activation energies can be ascribed to the distinct characteristics of the internal structure of FTs.

This study could identify the crystalline nature of MFTs, as opposed to the amorphous nature of ZFTs. Consequently, quenching in amorphizable materials, such as zircon, leads to the formation of amorphous structures, whereas quenching in non-amorphizable materials, such as monazite, leads to recrystallization during rapid cooling. The annealing process of FTs in monazite-(Ce) could be regarded as the recovery process of point defects arranged linearly along the ion path. As previously discussed, even if monazite-(Ce) areas are partially molten, they mainly recrystallize immediately during rapid cooling following spontaneous fission events. It is hypothesized that the annealing kinetics of linear point defects differ from those of amorphous areas. Crystallization of point defects may require lower energy for thermal activation compared to that for amorphous areas. This hypothesis is supported by

https://doi.org/10.5194/egusphere-2025-6112
Preprint. Discussion started: 30 March 2026

the observation that closure temperature of the MFT system is notably lower compared to other FT methods (as illustrated in Fig. 6).

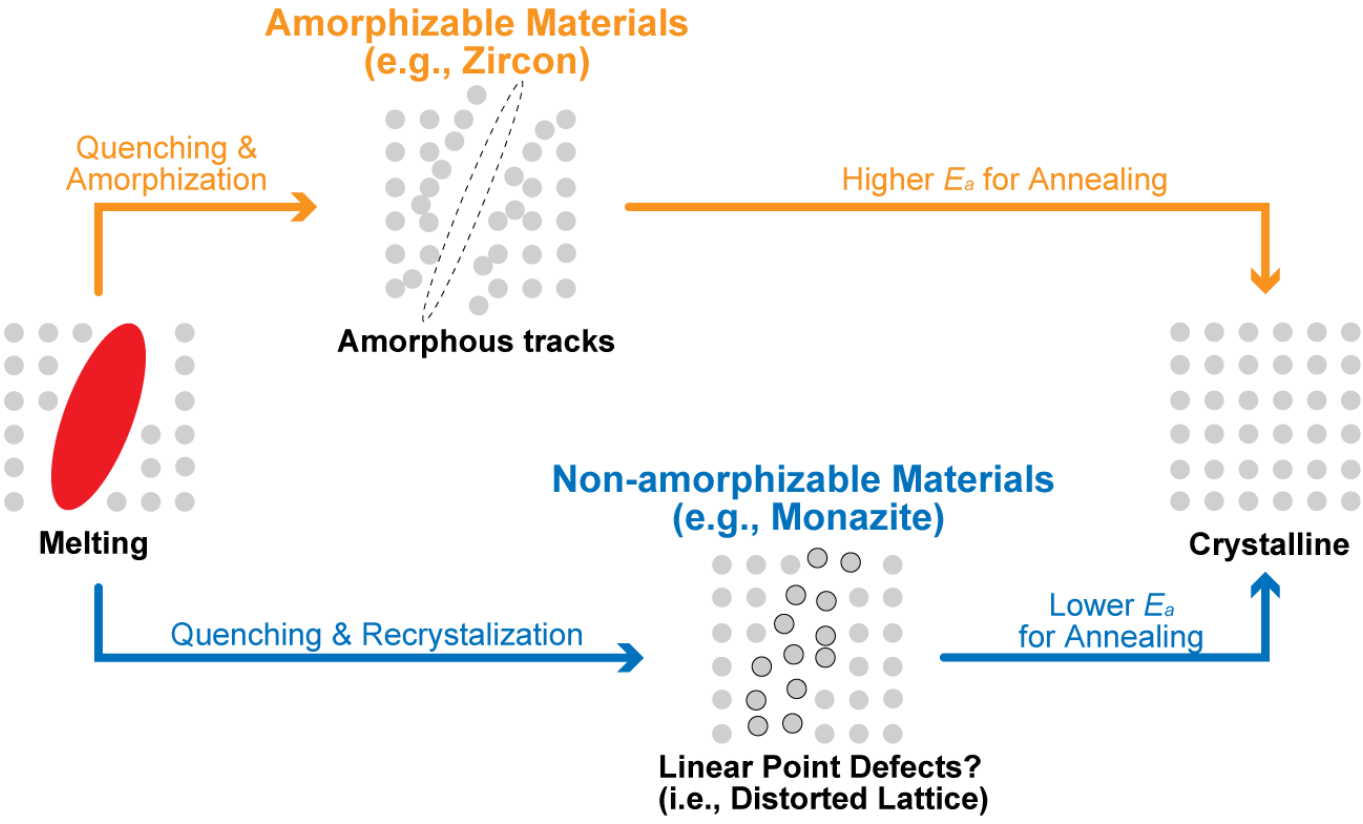

Fig. 6: A conceptual diagram of the possible fission-track creation and annealing process on crystalline structures in amorphizable (e.g., zircon) and non-amorphizable (e.g., monazite) materials. Gray particles denote atoms in each crystal. The closure temperature of the zircon FT system is estimated at ~300°C, while that of the monazite FT system is below 50°C, deducing that activation energies (E_a) for annealing may significantly differ between these materials.

5 Conclusions

This study considered the irradiation of Cretaceous monazite-(Ce) with Xe ions at 80 MeV and 200 MeV, as analogues of spontaneous fission. The resulting irradiation damage was then subjected to detailed observation using TEM. From the results, crystalline lattices remained within the ion track area at both energies, indicating the

https://doi.org/10.5194/egusphere-2025-6112
Preprint. Discussion started: 30 March 2026

occurrence of rapid recrystallization during rapid cooling after melting. On the other hand, TEM images of zircon showed amorphous structures as a result of Xe ion irradiation at 80 MeV. This observation differs from the outcome for monazite, despite the two samples being irradiated under the same conditions. Recrystallization in monazite may lead to the formation of point defects rather than amorphous regions along the ion path. As indicated by the findings of earlier investigations and this study, point defects can be chemically etched along the ion path in monazite. The substantially lower closure temperatures of the monazite fission-track system compared to other fission-track thermochronometers can be attributed to the formation of point defects within monazite, as opposed to the formation of amorphous regions. This is considered to support the hypothesis that point defects undergo facile thermal recovery, whereas the amorphous areas require a greater E_a to recover. For future prospects, further investigation, including TEM observations on other monazite groups (e.g., monazite-(Sm), as well as monazite-(La), monazite-(Nd)), using irradiation with various ion species, is desired.

Data availability

All data used in this study are presented in this manuscript.

Supplement

No supplemental data are provided.

Author contributions

SF and NI designed this study, the conceptual ideas, and the proof outline. TN obtained the rock sample of Toya-6b. SF and TN prepared the material. NI, HO, and TT conducted Xe irradiation and TEM observation. SF wrote the manuscript with support from NI and TN. All authors have read and agreed to publish this manuscript.

Competing interests

There are no competing interests to declare.

https://doi.org/10.5194/egusphere-2025-6112
Preprint. Discussion started: 30 March 2026

Acknowledgments

We would like to thank Dr. Hideki Iwano and Tohru Danhara (Kyoto Fission-Track Co. Ltd.) for conducting the monazite extraction of EY137-21 using general mineral separation techniques. EY137-21 was kindly provided by Shigeru Sueoka (Japan Atomic Energy Agency).

Financial support

This research was funded by the Ministry of Economy, Trade, and Industry, Japan, as part of its R&D support program "Research and development project for the geological disposal of high-level radioactive waste (Grant Number: JPJ007597; Fiscal Year 2024): Establishment of Technology for Comprehensive Evaluation of the Long-term Geosphere Stability on Geological Disposal Project of Radioactive Waste" .

References

Gilson, S. E., Svitlyk, V., Bukaemskiy, A. A., Niessen, J., Lender, T., Murphy, G. L., Henkes, M., Lippold, H., Marquardt, J., Akhmadaliev, S., Hennig, C., Winkler, B., Tonnesen, T., Peters, L., Fischeer, C., and Huittinen, N.: Microstructural investigation of Au ion-irradiated Eu-doped $LaPO_4$ ceramics and single crystals. npj Materials Degradation, 8(1), 83, doi.org/10.1038/s41529-024-00504-3, 2024.

Gleadow, A. J. W., Belton, D. X., Kohn, B. P. and Brown, R. W.: Fission Track Dating of Phosphate Minerals and the Thermochronology of Apatite, Rev. Mineral. Geochemistry, 48(1), 579–630, doi.org/10.2138/rmg.2002.48.16, 2002.

Goto, Y., Suzuki, K., Shinya, T., Yamauchi, A., Miyoshi, M., Danhara, T., and Tomiya, A.: Stratigraphy and lithofacies of the Toya Ignimbrite in southwestern Hokkaido, Japan: Insights into the caldera-forming eruption at Toya caldera. Journal of Geography (Chigaku Zasshi), 127(2), 191–227, doi.org/10.5026/jgeography.127.191, 2018.

Ishikawa, N., Chimi, Y., Michikami, O., Ohta, Y., Ohhara, K., Lang, M., and Neumann, R.: Study of structural change in CeO_2 irradiated with high-energy ions by means of X-ray diffraction measurement, Nucl. Instr. Meth. B 266 3033–3036. doi:10.1016/j.nimb.2008.03.159, 2008.

Ishikawa, N., Taguchi, T., and Okubo, N.: Hillocks created for amorphizable and non-amorphizable ceramics irradiated with swift heavy ions: TEM study, Nanotechnology, 28, 445708, doi:10.1088/1361 6528/aa8778, 2017.

https://doi.org/10.5194/egusphere-2025-6112
Preprint. Discussion started: 30 March 2026

Jepson, G., Carrapa, B., Jones, S., Kohn, B. P., Gleadow, A. J. W., George, S. W. M., Howlett, C. J., Gallagher, K., Frickenstein, A. N., Gehrels, G., Triantafyllou, A.: An assessment of monazite fission-track thermochronology as a proxy for low-magnitude cooling, Catalina-Rincon Metamorphic Core Complex, AZ, USA. Geochem. Geophys. Geosyst., 26, e2024GC011881. https://doi.org/10.1029/2024GC011881, 2025.

Jones, S., Gleadow, A. J. W., Kohn, B. P., and Reddy, S. M.: Etching of fission tracks in monazite: An experimental study, Terra Nova, 31(3), 179–188, doi:10.1111/ter.12382, 2019.

Jones, S., Gleadow, A. J. W., and Kohn, B. P.: Thermal annealing of implanted ^{252}Cf fission tracks in monazite, GChron, 3(1), 89–102, doi:10.5194/gchron-3-89-2021, 2021.

Jones, S., Kohn, B. P., Gleadow, A. J. W., Skrzypek, E., and Tagami, T.: Low-temperature thermochronology of Ryoke belt granitoids, SW Japan: New insights into the recent cooling history from monazite fission-track dating, Tectonophysics, 864, 229998, doi:10.1016/j.tecto.2023.229998, 2023.

Ketcham, R. A.: Fission-track annealing: from geologic observations to thermal history modeling, in *Fission-track thermochronology and its application to geology*, edited by Malusà, M. G.and Fitzgerald, P. G. pp. 49–76., doi.org/10.1007/978-3-319-89421-8_3, 2019.

Li, W., Wang, L., Lang, M., Trautmann, C., and Ewing, R. C.: Thermal annealing mechanisms of latent fission tracks: Apatite vs. zircon, Earth Planet. Sci. Lett., 302(1–2), 227–235, doi:10.1016/j.epsl.2010.12.016, 2011.

Nakajima, T., Fukuda, S., Sueoka, S., Niki, S., Kawakami, T., Danhara, T., and Tagami, T.: Short communication: Inverse correlation between radiation damage and fission-track etching time on monazite, GChron, 6(3), 313–323, doi:10.5194/gchron-6-313-2024, 2024.

Nasdala, L., Akhmadaliev, S., Burakov, B. E., Chutimun, C. and Škoda, R.: The absence of metamictisation in natural monazite, Sci. Rep., 10:14676, 1–9, doi:10.1038/s41598-020-71451-7, 2020.

Overstreet, C., Cooper, J., Quinn, E. O., Cureton, W., Palomares, R., Leys, J., Deissmann, G., Neumeier, S., Chen, C., and Lang, M.: Structural stability of REE-PO_4 (REE = Sm, Tb) under swift heavy ion irradiation, Nucl. Inst. Methods Phys. Res. B, 527, 34–39, doi:10.1016/j.nimb.2022.07.014, 2022.

Rymzhanov, R.A., Medvedev, N., O'Connell, J.H., Janse van Vuuren, A., Skuratov, V.A., and Volkov, A.E.: Recrystallization as the governing mechanism of ion track formation, Sci. Rep., 9:3837, doi.org/10.1038/s41598-019-40239-9, 2019.

Seydoux-Guillaume, A.-M., Wirth, R., Deutsch, A. and Schärer, U.: Microstructure of 24-1928 Ma concordant monazites; implications for geochronology and nuclear waste deposits, Geochim. Cosmochim. Acta, 68(11), 2517–2527, doi:10.1016/j.gca.2003.10.042, 2004.

https://doi.org/10.5194/egusphere-2025-6112
Preprint. Discussion started: 30 March 2026

Skrzypek, E., Kawakami, T., Hirajima, T., Sakata, S., Hirata, T., and Ikeda, T.: Revisiting the high temperature metamorphic field gradient of the Ryoke Belt (SW Japan): New constraints from the Iwakuni-Yanai area, Lithos, 260, 9–27, doi:10.1016/j.lithos.2016.04.025, 2016.

Tagami, T., and O'Sullivan, P. B.: Fundamentals of fission-track thermochronology, Rev. in Min. Geochem., 58(1), 19–47, doi.org/10.2138/rmg.2005.58.2, 2005.

Takaki, S., Yasuda, K., Yamamoto, T., Matsumura, S. and Ishikawa, N.: Structure of ion tracks in ceria irradiated with high energy xenon ions, Prog. Nucl. Energy, 92, 306–312, doi:10.1016/j.pnucene.2016.07.013, 2016.

Trautmann, C., Schwartz, K., Geiss, O.: Chemical etching of ion tracks in LiF crystals, Jour. Appl. Physic., 83(7), 3560–3564, 1998.

Tomiya, A. and Miyagi, I.: Age of the Toya eruption, Bull. Volcanol. Soc. Japan, 65, 13–18, 2020 (in Japanese).

Toulemonde, M., Assmann, W., Dufour, C., Meftah, A., Trautmann, C.: Nanometric transformation of the matter by short and intense electronic excitation: Experimental data versus inelastic thermal spike model. Nucl. Instrum. Methods Phys. Res. Sect. B Beam Interact. Mater. Atoms, 277, 28–39. https://doi.org/10.1016/j.nimb.2011.12.045, 2012.

Szenes, G.: Comparison of two thermal spike models for ion–solid interaction. Nucl. Instrum. Methods Phys. Res. Sect. B: Beam Interact. Mater. Atoms 2011, 269, 174–179, doi.org/10.1016/j.nimb.2010.11.009, 2011.

Yada, K., Tanji, T. and Sunagawa, I.: Radiation induced lattice defects in natural zircon ($ZrSiO_4$) observed at atomic resolution, Phys Chem Minerals, 14, 197–204, doi.org/10.1007/BF00307984, 1987.

Yamada, R., Tagami, T., and Nishimura, S.: Confined fission-track length measurement of zircon: assessment of factors affecting the paleotemperature estimate. Chem. Geol., 119(1-4), 293–306, doi.org/10.1016/0009-2541(94)00108-K, 1995.

Weise, C., Boogaart, K. G. Van Den, Jonckheere, R. and Ratschbacher, L.: Annealing kinetics of Kr-tracks in monazite: Implications for fission-track modelling, Chem. Geol., 260, 129–137, doi:10.1016/j.chemgeo.2008.12.014, 2009.